ORIGINAL ARTICLE

Comparison and integration of CONT17 networks

Younghee Kwak[1] · Matthias Glomsda[1] · Detlef Angermann[1] · Michael Gerstl[1]

Abstract

Among the continuous (CONT) campaigns of very long baseline interferometry (VLBI), CONT17 is a special CONT campaign which comprises three independent networks: two legacy networks, and one VGOS network to mainly check possible biases in network geometry. In this study, we estimate all types of geodetic parameters (station and source coordinates, and Earth orientation parameters (EOP)) within the single networks and compare them to investigate potential network dependent biases. Since the separate networks are technically linked to each other by common parameters, i.e. EOP and common radio source coordinates, they can be regarded as a single network on the Earth and integrated in one common adjustment. Thus, we also estimate the station and source coordinates, and the EOP from the integrated networks and compare them with those of the single networks to check the impact on the geodetic parameters. There are both subtle and large biases (up to 7.1 mm between the legacy networks in the Ty component and 23.3 mm between the legacy and VGOS networks in the D_3 component on the surface of the Earth) between the single networks depending on parameter types. The integrated network eventually compensates those differences. Adding the VGOS network to the legacy networks does not show any significant improvement for the latter. However, the integration can provide the VGOS network with better parameter estimates which is important for the new stations.

Keywords CONT17 · VLBI · Network comparison · Network integration · TRF · EOP · CRF

1 Introduction

The general very long baseline interferometry (VLBI) sessions have not been continuous, mainly due to the limitation of human/hardware/software resources and/or other tasks for astronomy at most VLBI stations. Following successful continuous VLBI (CONT) campaigns which were conducted only at irregular intervals since 1994, the International VLBI Service for Geodesy and Astrometry (IVS) has organized CONT campaigns in three-year intervals since 2005. The CONT campaign is a valuable session series, which can contribute to new VLBI observation and analysis strategies as well as hardware development, even though it only lasts for 2 weeks. The latest CONT campaign is CONT17, which was conducted in November and December of 2017 (28-NOV-2017 00:00 UT through 12-DEC-2017 24:00 UT). CONT17 is unique because it has three different networks, two legacy

ones and a VLBI Global Observing System (VGOS; Petra-chenko et al. 2012) network.

In this study, we analyze all geodetic parameters (station and source coordinates, and Earth orientation parameters (EOP)) for the single networks and compare them to investigate possible network dependent biases. Furthermore, we integrate all three single networks and discuss the impact of the integration on the geodetic parameters.

In the following, Sect. 2 briefly introduces the CONT17 legacy and VGOS networks, and Sect. 3 describes how we set up the respective solutions. Section 4 deals with the analysis of the single CONT17 networks, including parameter estimation and their comparison. Section 5 discusses the integrated network. Lastly, Sect. 6 summarizes the results and draw the conclusions.

2 CONT17 networks

CONT17 consists of two legacy networks and one VGOS network, see Table 1 and Fig. 1.

✉ Younghee Kwak
  younghee.kwak@tum.de

[1] Deutsches Geodätisches Forschungsinstitut at the Technische Universität München (DGFI-TUM), Arcisstr. 21, 80333 Munich, Germany

Table 1 Participating stations in CONT17. SC-VLBA could not participate in CONT17 due to a hurricane damage

Name	Code	Observatory name and location
Legacy-1 (XB)		
BADARY	Bd	Badary Radio Astronomical Observatory, Russia
FORTLEZA	Ft	Space Radio Observatory of the Northeast (ROEN), Fortaleza, Brazil
HART15M	Ht	Hartebeesthoek Radio Astronomy Observatory, South Africa
HOBART26	Ho	Mt. Pleasant Radio Astronomy Observatory, Hobart, TAS, Australia
KASHIM11	K1	Kashima VLBI Station, Japan
KATH12M	Ke	Katherine Observatory, Katherine, NT, Australia
KOKEE	Kk	Kokee Park Geophysical Observatory, Kauai, HI, USA
MATERA	Ma	Centro di Geodesia Spaziale G. Colombo, Matera, Italy
NYALES20	Ny	Ny Ålesund Geodetic Observatory, Spitsbergen, Norway
ONSALA60	On	Onsala Space Observatory, Sweden
WARK12M	Ww	Warkworth VLBI Station, New Zealand
WETTZELL	Wz	Geodetic Observatory Wettzell, Germany
YEBES40M	Ys	Astronomical Center at Yebes, Spain
ZELENCHK	Zc	Radioastronomical Observatory Zelenchukskaya, Russia
Legacy-2 (XA)		
BR-VLBA	Br	VLBA Station, Brewster, WA, USA
FD-VLBA	Fd	VLBA Station, Ft. Davis, TX, USA
HN-VLBA	Hn	VLBA Station, Hancock, NH, USA
KP-VLBA	Kp	VLBA Station, Kitt Peak, AZ, USA
LA-VLBA	La	VLBA Station, Los Alamos, NM, USA
MK-VLBA	Mk	VLBA Station, Mauna Kea, HI, USA
NL-VLBA	Nl	VLBA Station, North Liberty, IA, USA
OV-VLBA	Ov	VLBA Station, Owens Valley, CA, USA
PIETOWN	Pt	VLBA Station, Pie Town, NM, USA
SC-VLBA	Sc	VLBA Station, St. Croix, VI, USA
MEDICINA	Mc	Medicina Radio Astronomy Station, Italy
SESHAN25	Sh	Shanghai Astronomical Observatory, Seshan, China
WETTZ13N	Wn	Geodetic Observatory Wettzell, Germany
YARRA12M	Ya	Yarragadee Observatory, Yarragadee, WA, Australia
VGOS (VG)		
GGAO12M	Gs	Westford Antenna, Haystack Observatory, MA, USA
ISHIOKA	Is	Ishioka VLBI Station, Japan
KOKEE12M	K2	Kokee Park Geophysical Observatory, Kauai, HI, USA
WESTFORD	Wf	Westford Antenna, Haystack Observatory, MA, USA
WETTZ13S	Ws	Geodetic Observatory Wettzell, Germany
RAEGYEB	Yj	Astronomical Center at Yebes, Spain

The legacy network has 9 Very Long Baseline Array (VLBA) stations and 4 geodetic IVS stations, and the other legacy network consists of 14 geodetic IVS stations. The respective session codes are XA and XB. The XA network has only one station in the southern hemisphere (YARRA12M), and most of the stations are located in North America. In contrast to that, the XB network provides a more globally balanced distribution, except for North America.

The VGOS network only observed for five days / sessions (03-DEC-2017 23:00 UT through 08-DEC-2017 24:00 UT) during CONT17. Most of the time, it consisted of 5 stations: GGAO12M, ISHIOKA, KOKEE12M, WESTFORD, and WETTZ13S. Only in the first session, it was extended by RAEGYEB, which experienced a problem with antenna pointing for the four last sessions. Unfortunately, all of these stations are located in the northern hemisphere, so with respect to global distribution the situation is even worse than for the first legacy network XA. However, the main purpose of the VGOS sessions (code VG) was a demonstration of VGOS' current capabilities. In contrast to the legacy
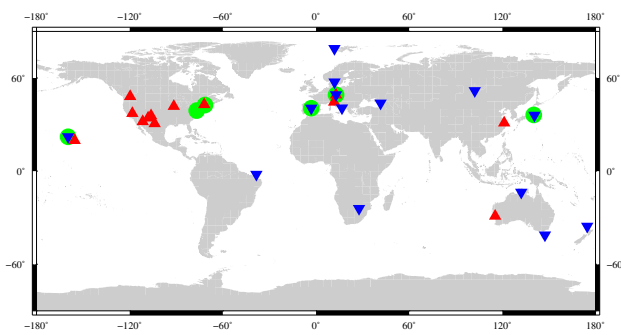
Fig. 1 CONT17 networks. The red up-pointing triangles represent 9 VLBA stations and 4 geodetic IVS stations. The blue down-pointing triangles depict 14 geodetic IVS stations. The green dots are 6 VGOS stations. The IVS observation codes corresponding to these three networks are XA, XB, and VG, respectively

S/X-band observations, the VGOS stations observe a broadband delay, which shall lead to an improved delay precision. By using smaller and faster-slewing antennas, as well as by reducing the scan duration, many more scans per session are possible. The first four VGOS sessions during CONT17 lasted for 24 hours, the last one for 25 hours.

For more details of CONT17, please see the website: https://ivscc.gsfc.nasa.gov/program/cont17/.

3 Solution setups

Three sets of network-dependent VLBI observations were processed/analyzed with DGFI-TUM's in-house VLBI software: DGFI Orbit and Geodetic parameter estimation Software - Radio Interferometry (DOGS-RI; Kwak et al. 2017). The outputs of DOGS-RI were datum-free normal equations in which the troposphere and clock parameters were reduced.

In this paper, we deal with three types of solutions: (1) session-wise solutions for the single networks, (2) global solutions for the single networks, and (3) a global solution for the integrated network. The session-wise solutions correspond to the daily solutions of the IVS and therefore include station and source coordinates and EOPs at midnight. The global solutions are multi-session solutions, whose estimated parameters are constant station and source coordinates for 15 days and an EOP time-series (at every midnight). For more details of the models, a priori values, and parameterization, see Table 2. The advantage of the global solution is that more data points can be used in the parameter estimation for EOPs as well as station and source coordinates. The global solution of the integrated network is estimated in the same way as for the single-network global solutions, except for using the integrated normal equations of the three single networks. It should be noted that, in all solutions of this paper, the estimated parameters were adjusted simultaneously to keep

the consistency between the terrestrial and celestial frames (IUGG 2011; Kwak et al. 2018).

Most stations of the VG network are new and their a priori station coordinates were not accurate enough. Therefore, we re-estimated the parameters using adjusted a priori station coordinates from the first integration.

In order to integrate the three independent networks, and to keep the consistency between the single networks and the integrated network, time series analyses and global solutions were performed with the DGFI Orbit and Geodetic parameter estimation Software - Combination and Solution (DOGS-CS; Gerstl et al. 2000; Angermann et al. 2004). Because we analyze VLBI-only observations, no-net-translation (NNR) and no-net-rotation (NNT) conditions w.r.t. ITRF2014 (Altamimi et al. 2016) and a NNR condition w.r.t. ICRF3 (Charlot et al. 2020) were applied to avoid singularities in all solutions.

4 Analysis of single CONT17 networks

4.1 Station coordinates

In order to check the bias in network geometry directly, the time series (session-wise estimation) of the parameters of a Helmert transformation w.r.t. ITRF2014 are investigated. As the stations of the VGOS network are very new and most of them are not included in the ITRF2014, the VGOS network is not addressed in this subsection.

Figure 2 depicts the time series of translation (Tx, Ty, and Tz), rotation (Rx, Ry, and Rz), and scale during the 15 days of CONT17. The direct comparison of the Helmert transformation w.r.t. ITRF2014 is not very significant because the NNR/NNT conditions w.r.t. ITRF2014 were already given during estimation. The steadiness of the time series is more meaningful. However, depending on the network configuration (geometry and participating stations), there could also be additional translations and rotations.

There are unexpected offsets in translation and scale parameters at DOY 342. They stem from the HN-VLBA station. However, no problems have been reported for HN-VLBA in the corresponding session, and the reason is still under investigation.

The rotations of the XA network imply less deviation to ITRF2014 than the XB network. In the XA network, most stations contribute to the ITRF2014 with a long-period of data. On the other hand, some stations of the XB network have shorter observation time spans and thus less contribution to ITRF2014, e.g. KATH12M and WARK12M. This results in a consistent offset for several Helmert parameters (Tx, Ty, Tz, Rx, Rz) w.r.t. ITRF2014 in the XB network. Nevertheless, the steadiness of the translation and scale parameters is stronger than for the XA network, and it implies that a balanced global

Table 2 Major models, a priori values, and parameterization in the session-wise and global solutions

	Model
Precession/Nutation	IAU2006A
Tidal effects	IERS2010

	A priori
TRF	ITRF2014 (Altamimi et al. 2016)
	Adjusted coordinates after the first integration (VGOS stations not in ITRF2014; Table 3)
EOP	IERS 14 C04 (Bizouard et al. 2019)
CRF	ICRF3 (Charlot et al. 2020)

	Parameters	**Interval**
Station clocks	Piecewise linear (pwl) offsets	1 h
	Clock rate and quadratic term	24 h (1/session)
Zenith wet delays	pwl offsets	1 h (legacy)
		0.25 h (VGOS)
Troposphere gradients	pwl east and north components	24 h (legacy)
		1h (VGOS)
EOP	pwl x-pole, y-pole, dUT1	24 h (at 0:00UTC)
	dX, dY	24 h (at the middle of the session)
Station coordinates	NNR/NNT condition w.r.t. ITRF2014	24 h (1/session) for session-wise solutions
	on selected datum stations	1/15 days (legacy) or 1/5 days (VGOS) for global solutions
Source coordinates	NNR condition w.r.t. ICRF3	24 h (1/session) for session-wise solutions
	on defining sources	1/15 days (legacy) or 1/5 days (VGOS) for global solutions

The clock and troposphere parameters were pre-reduced

Table 3 Adjusted a priori coordinates of VGOS stations not in ITRF2014 after the first integration[a]. The units are meters. The reference epoch is 2017-12-05 12:00UTC

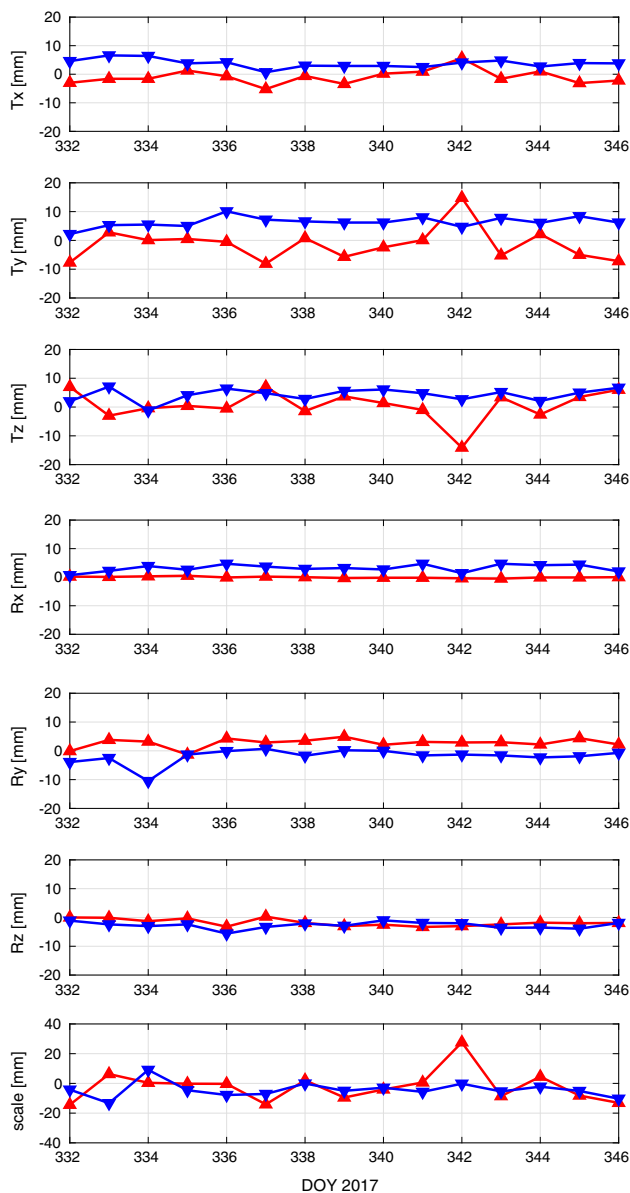| Station	X	Y	Z
RAEGYEB	4 848 831.0539	−261 629.4399	4 122 976.5394
WETTZ13S	4 075 658.8908	931 824.8538	4 801 516.2806
ISHIOKA	−3 959 636.1430	3 296 825.4740	3 747 042.5991
KOKEE12M	−5 543 831.7485	−2 054 585.7607	2 387 828.8940
GGAO12M	1 130 729.9021	−4 831 245.9597	3 994 228.2859

[a] opa2019a for the first run

distribution enables a better determination of the translation and scale parameters.

Figure 3 shows the Helmert transformation parameters (translation, rotation, and scale) w.r.t. ITRF2014 for the single XA and XB networks (and the integrated network, compare below) based on global solutions. Overall, the Helmert transformation parameters of the global solutions w.r.t. ITRF2014 reflect the average behaviour of the session-wise solutions. The maximum difference between the legacy networks is 7.1 mm at the Ty component. In contrast to the XB network, the TRF estimated by the XA network follows ITRF2014 well, because most stations of the XA network were strongly involved in the generation of ITRF2014 as described in the previous paragraph. Except for the Ry component, the Helmert parameters of the XA network have a value below 2 mm.

4.2 EOP time series

Figure 4 shows the time series of EOP offsets w.r.t. IERS 14 C04 (Bizouard et al. 2019) during CONT17 from session-wise and global solutions of the networks XA and XB, respectively. In the session-wise solutions, x-pole, y-pole, and dUT1 at every midnight (session boundary) are estimated, and usually the EOP from separate sessions do not perfectly match each other at the session boundary as shown in Fig. 4. There are larger standard deviations in dX and dY for the XA network at DOY 342. They coincide with the time series offsets of the translation and scale parameters in Fig. 2. However, those effects were suppressed in the global solution.
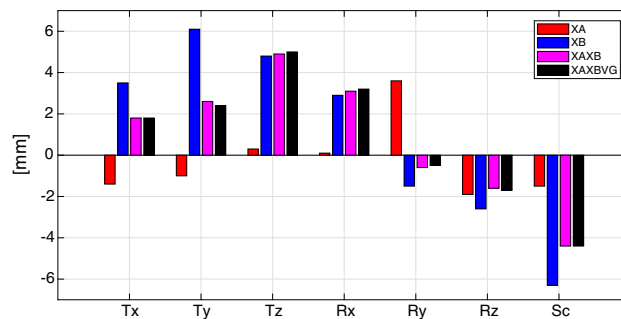
On the other hand, the EOP series from the global solutions are more stable than from the session-wise solutions. The

Fig. 2 Time series of translation, rotation, and scale offsets of session-wise solutions (red up-pointing triangle for XA network and blue down-pointing triangle for XB network) w.r.t. ITRF2014. The rotation components are projected values on the Earth surface for better understanding

Fig. 3 Estimated Helmert transformation parameters (translation: Tx, Ty, and Tz; rotation: Rx, Ry, and Rz; scale: Sc) for the global solutions of the XA (first red bars), XB (second blue bars), and integrated (third magenta bars only for legacy networks and fourth black bars for all the networks) networks w.r.t. ITRF2014. The rotation components are projected values on the Earth surface for better understanding

networks are 5.7, 24.6, 8.9, 10.5 μas, and 4.3 μs on average for the wmean values of x-pole, y-pole, dX, dY, and dUT1, respectively. These differences correspond to 0.2–0.7 mm on the surface of the Earth. X-pole, dX, and dY agree with IERS 14 C04 slightly better in the XA network, whereas y-pole and dUT1 agree better in the XB network. Hence, it is hard to assess which network has the better configuration for EOP determination. However, the XB network has better east-west distribution, which is important for dUT1 determination, and its dUT1 shows better agreement with the one of IERS 14 C04. Therefore, the XB network benefits dUT1 at least.

The EOP were critical in the VG network. As most stations are new and their a priori station coordinates are not accurate enough, huge wmean offsets appeared for x-pole, y-pole, and dUT1 (-1439.5 and 6674.5 μas and 64.7 μs, respectively; not shown in this paper) in the first estimation. The maximum difference for wmean between VGOS and the legacy networks was 204.2 mm (on the surface of the Earth) for y-pole. dY also showed a large disagreement (-537 μas) with IERS 14 C04, likely due to the small and northern hemisphere biased network configuration and thus insufficient estimation of source coordinates, while dX was estimated in a reasonable range. Therefore, we re-estimated the parameters using the adjusted station coordinates from the first integration. The new x-pole, y-pole, and dUT1 of the VG networks show better agreement w.r.t. the IERS 14 C04 than the legacy networks in Fig. 5. dX has a different direction compared to the ones of the legacy networks while dY is comparable with the ones of the legacy networks. The limited number of radio sources of the VG network likely caused such a reversal. More details are described in Sect. 4.3. The WRMS values for the VG network (except dY) are better than those for the legacy networks because of its new type of broadband data and the larger amount of scans regardless of the a priori station coordinates.

EOP of the session-wise solutions are estimated from fewer data points in a shorter time span (based on only one session) than the ones of the global solutions. The standard deviations of the EOP in the global solutions are also much smaller than those of the session-wise solutions mainly due to the greater amount of data.

In general, both legacy networks show comparable quality, i.e. weighted mean (wmean) and weighted root-mean-square (WRMS) values, when their EOP estimates are compared with IERS 14 C04 (Fig. 5). The differences between the two

Fig. 4 Time series of EOP offsets (left panels), i.e. *x*-pole, *y*-pole, dUT1, and x and y components of celestial offsets (dX and dY), w.r.t. IERS 14 C04 from session-wise and global solutions of the XA and XB networks, and their corresponding standard deviations (right panels). Magenta asterisk and cyan square lines indicate the session-wise solutions for the XA and XB networks, respectively. Red circle and blue diamond lines represent the global solutions for XA and XB networks, respectively

4.3 Source coordinates

Due to the network configuration, the observable radio sources are limited, as shown in Fig. 6. The XA network, which mostly consists of the VLBA network in North America, was only able to observe the radio sources with a declination of up to 50 degrees in the southern hemisphere, while the XB network could even observe sources near the South pole. The VG network only consists of 5-6 stations, all located in the northern hemisphere, and thus it can only observe (sparsely distributed) sources with a declination of less than 30 degrees in the southern hemisphere.

When we compare the source coordinates w.r.t. ICRF2 (Fey et al. 2015), there is a declination bias (Mayer et al. 2017) in the XB network only (not shown in this paper), which has southern hemisphere stations, i.e. HOBART26, KATH12M, and WARK12M, even though there are 45 common sources in both legacy networks. On the other hand, when we compare the source coordinates derived from the XB network to those of ICRF3 (Fig. 7), which is the latest official version of the International Celestial Reference Frame (ICRF), the bias becomes smaller than the one w.r.t. ICRF2 even though it is still large (-114.7 μas). The right ascensions did not show any specific characteristics, neither in the XA nor XB network. The VG network shows less accurate estimates of the source coordinates (Fig. 7) which is normal due to the sparse and north-biased distribution. This defect is also transferred to the celestial pole offsets, especially dX (Fig. 5). However, after integration with the XA and XB networks, it is compensated as described in Sect. 5.2 and 5.3.

More comparisons using the vector spherical harmonics (VSH) decomposition are discussed in Sect. 5.3 together with the integrated network.

5 Analysis of integrated CONT17 network

The XA, XB, and VG networks partly have common parameters, i.e. common radio sources (45 between XA and XB; 33 between XA and VG; 32 between XB and VG; 43 between XA+XB and VG) and EOP. Therefore, it is worthwhile to try to integrate the three networks and jointly estimate the common parameters to make the best use of the available observation sets.

As there are common EOPs and some common radio sources with NNR conditions w.r.t. ICRF3, and hence sufficient condition equations for rotation during integration of the three networks, the rotational singularity could be resolved. However, the three networks are consisting of entirely separate station sets, and no more constraints were
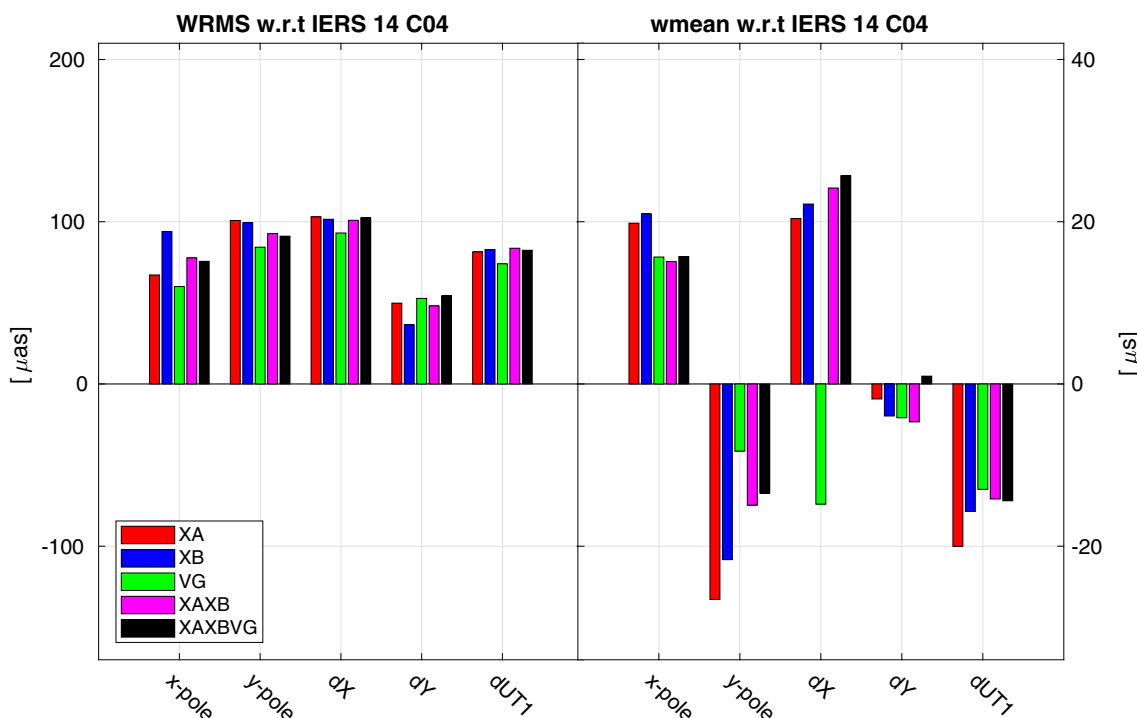
Fig. 5 EOP comparison of the XA (first red bars), XB (second blue bars), VG (third green bars), and integrated (fourth magenta bars only for legacy networks and fifth black bars for all the networks) networks w.r.t. the IERS 14 C04 time series. The EOP are from the global solutions.

The left panel shows the weighted root-mean-square values (WRMS); the right panel shows the weighted mean (wmean) values. The left vertical axis denotes the scale of *x/y*-pole and dX/dY, and the right one indicates that of dUT1

given other than NNR/NNT conditions w.r.t. ITRF2014 to not distort the single network geometries. As a consequence, the integrated system becomes (almost) singular due to the lack of translational connections between the three separate equation systems. To overcome this translational singularity, the local ties (5 pairs) at the co-located sites were introduced: WETTZ13N(XA) - WETTZELL(XB), WETTZ13N(XA) - WETTZ13S(VG), WETTZELL(XB) - WETTZ13S(VG), KOKEE(XB) - KOKEE12M(VG), YEBES40M(XB) - RAE-GYEB(VG). The values and data sources of the local ties are listed in Table 4.

5.1 Station coordinates

As mentioned in Sect. 4.1, most stations of the VGOS network are not included in the ITRF2014. Hence, the Helmert transformation parameters are compared for XA, XB, the integrated network of XA and XB (XAXB), and the integrated network of XA, XB and VG (XAXBVG).

Both integrated networks (XAXB and XAXBVG) cancel the differences between the two legacy networks to some extent for most components. The translation (except Tz) and scale parameters of the integrated networks are close to averages of (or somewhere in between) those of the two legacy networks (Fig. 3). The integrated networks have less rotation

in *y* and *z* direction than both single legacy networks, and the rotation in *x* direction is almost the same as for the XB network. As seen from the time series in Fig. 2, a small difference does not mean better results. Even though there are larger offsets, steadiness could be preferable.

In all solutions, NNR/NNT conditions were applied, and only the scale parameter was intrinsically determined. Depending on network geometry, the scale parameter varies by up to 4.8 mm (between the global solutions for XA and XB networks, Fig. 3). This means that the network distribution (selection of a network) should be considered carefully during the preparation of VLBI sessions, because the intrinsic VLBI scale plays an important role in the generation of the International Terrestrial Reference Frame (ITRF).

As mentioned Sect. 4.2, most VGOS stations are new and/or have non-optimal a priori values for station coordinates and therefore caused large offsets at several EOP components. After integrating the XA, XB, and VG networks, the station coordinates of the VG network were significantly adjusted by up to 44.2 cm (GGAO12M; not shown in this paper) even though the Helmert transformation parameters between the XAXB and XAXBVG networks do not show any big difference. When we applied the adjusted a priori values, the EOP of the single VG network became reasonable as shown in Fig. 5.

Table 4 The local ties at the co-located sites. The units are meters

Local tie	X	Y	Z
WETTZ13N (XA) - WETTZELL (XB)[a]	88.0364	38.7315	−77.1628
WETTZ13N (XA) - WETTZ13S (VG)[a]	−31.3081	−50.5045	36.1315
WETTZELL (XB) - WETTZ13S (VG)[a]	−119.3444	−89.2359	113.2943
KOKEE (XB) - KOKEE12M (VG)[b]	−6.0720	19.2141	23.7230
YEBES40M (XB) - RAEGYEB (VG)[c]	−69.2923	145.3433	108.5589

[a]http://itrf.ign.fr/local_surveys.php
[b]https://www.ngs.noaa.gov/corbin/iss/reports/Kauai_Report_2018.pdf
[c]http://www1.oan.es/reports/doc/IT-CDT-2018-20.pdf
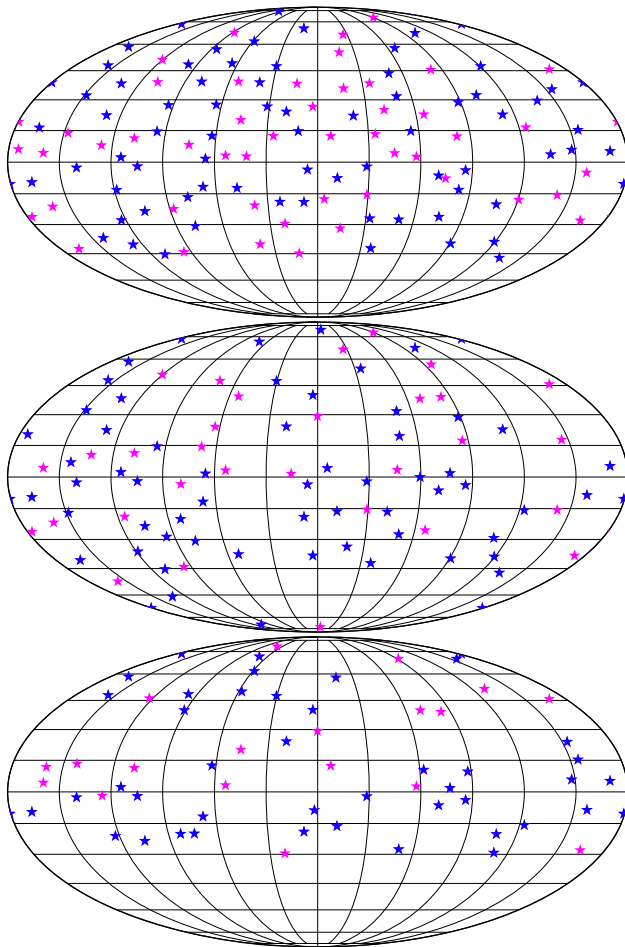
Fig. 6 Radio source maps which were observed by XA (first panel), XB (second panel), and VG (third panel) networks. Blue stars depict the defining sources, and magenta stars represent the other sources. The source coordinates and the list of defining sources are from ICRF3

5.2 EOP time series

Figure 5 depicts the WRMS and wmean values of the differences of the estimated EOP time series (global solutions) from XA, XB, VG, and the integrated networks (XAXB and XAXBVG) w.r.t. the IERS 14 C04 series, which is the latest

official EOP series. It reflects the EOP results when using adjusted a priori station coordinates for the VG network.

The WRMS of the EOP components are mostly comparable for the two legacy and integrated networks, while the WRMS of the VG network are even smaller than those of the integrated networks (Fig. 5). On the other hand, the wmean values of the five time series w.r.t. IERS 14 C04 show more variation depending on the networks. The integrated networks (XAXB and XAXBVG) show better agreement than the legacy networks for x-pole, y-pole, and dUT1. At least for the legacy networks, integrating the networks would benefit Earth rotation parameters, i.e. x-pole, y-pole, and dUT1, rather than celestial pole offsets. Adding the VG network to the two legacy networks does not harm to the EOP of the integrated legacy network, but it shows no significant improvement in terms of any wmean value, either, except dY (Fig. 5).

As mentioned in Sect. 4.2, due to inaccurate a priori values of the station coordinates in the VG network, there were large offsets in all the EOP except dX in the first estimation (not shown in this paper). Nevertheless, after integrating all three networks, these large offsets are drastically reduced (by up to 203.3 mm on the Earth surface). It means that integrating can provide better adjustments especially for the new stations which have rough a priori values.
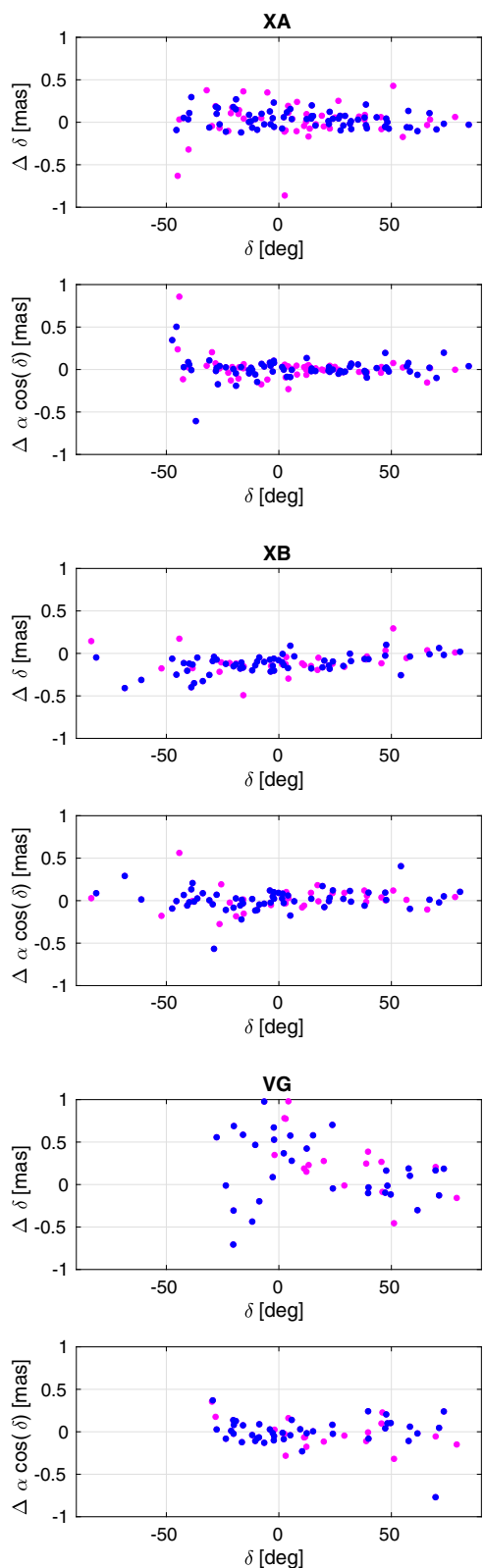
5.3 Source coordinates

To compare two different astrometric catalogs, the VSH decomposition, which still is an up-to-date method, was introduced (see Mignard and Klioner (2012); Titov and Lambert (2013)). The difference between two Celestial Reference Frames (CRFs) is represented as a vector field on a sphere:

$$\Delta\alpha\cos\delta = R_1\cos\alpha\sin\delta + R_2\sin\alpha\sin\delta - R_3\cos\delta$$
$$- D_1\sin\alpha + D_2\cos\alpha$$
$$+ \text{2nd order terms (quadrupole)}, \quad (1)$$
$$\Delta\delta = -R_1\sin\alpha + R_2\cos\alpha - D_1\cos\alpha\sin\delta$$
$$- D_2\sin\alpha\sin\delta + D_3\cos\delta$$
$$+ \text{2nd order terms (quadrupole)}, \quad (2)$$

Fig. 7 Source coordinate differences w.r.t. ICRF3. Odd panels: declinations from the XA, XB, and VG networks, respectively. Even panels: right ascensions from the XA, XB, and VG networks, respectively. Blue dots depict the defining sources, and magenta dots represent the other sources

where α and δ are the right ascension and declination of the source coordinates, respectively, and $\Delta\alpha$ and $\Delta\delta$ are the differences of the former between the two CRFs. The first degree terms in Eqs. (1) and (2), which have R_1, R_2, R_3, D_1, D_2 and D_3 coefficients, are linked to global features, i.e. rotation between the two CRFs and systematic dipole displacement (called *glide* in Mignard and Klioner (2012)). The higher degree terms describe the regional differences (for a more detailed mathematical expression, see Mignard and Klioner (2012); Titov and Lambert (2013)). In this paper, we focus on the comparison of the global components.

As expected from Fig. 7 and Sect. 4.3, the rotation and glide w.r.t. ICRF3 depend on the network.

The XB network (blue in Fig. 8), which observes more radio sources in the Southern hemisphere, does not have large rotations w.r.t. ICRF3. On the other hand, the North America biased network XA (red in Fig. 8) has a rotation (1.7 mm on the Earth surface) in R_1 direction. The limited distribution of the radio sources in declination likely promotes the rotation in R_1 and R_2 directions, even though the NNR conditions were applied during estimation. According to Eq. 1, the R_3 rotation is only associated with right ascension. Therefore, R_3 rotations in both legacy network are only small, implying a good agreement with ICRF3. The VG network, which is small and solely consists of northern stations, has huge R_1 rotation (173.8 μas; out of range in Fig. 8), while the R_2 and R_3 rotations are relatively small. The R_1 rotation of the legacy integrated network shows about the average rotation of two legacy network. The large R_1 rotation of the VG network likely impacts on the integrated legacy network to some extent. In both integrated networks, the R_2 rotations are comparable with the one of the XA network while the R_3 rotations are comparable with the one of the XB network. The VG network seldom affects the R_2 and the R_3 of the integrated legacy network.

In both legacy networks, the D_1 components do not have large values and the same holds for the integrated networks. The VG network has an offset (-80.2 μas) in the D_1 component. There are decent glides in the D_2 components for every network, only the VG network shows a different direction of offset. The D_3 component has a relatively large value (around 130 μas, which corresponds to 3.9 mm on the Earth surface) in the XB network. Based on the Eq. 2, we regard the D_3 component as an adjusted declination bias which is solely determined by the declination difference and declination. Moreover, the VG network has an extremely huge bias (645.9 μas; out of range in Fig. 8), which is obvious given the differences for the declination in Fig. 7. However, the integration of the three networks is clearly able to compensate the adjusted declination bias (D_3). The results induce a very promising aspect: a globally distributed network can clear all the (adjusted) declination biases even though it is integrated on the normal equation level and observed for only 15 days
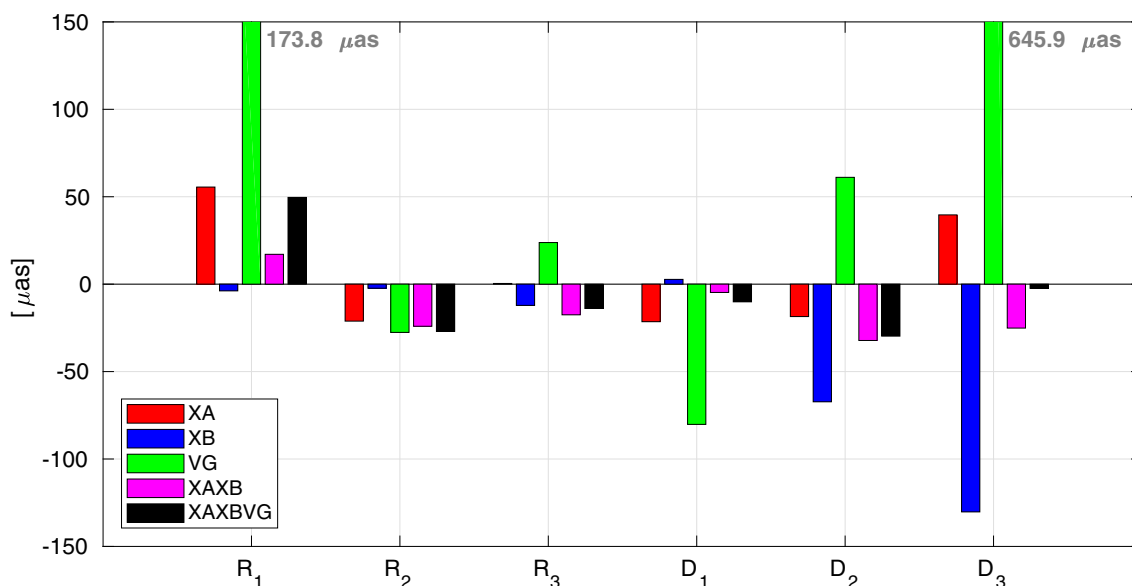
Fig. 8 VSH global components of the XA (first red bars), XB (second blue bars), VG (third green bars), and integrated (fourth magenta bars only for legacy networks and fifth black bars for all the networks) net- works w.r.t. ICRF3. R_1, R_2 and R_3 are rotations; D_1, D_2 and D_3 are glides (systematic dipole displacements)

(considering that the ICRF3 is based on more than 30 years of data).

6 Conclusions

The CONT17 campaign consists of two legacy networks and one VGOS network (session codes XA, XB, and VG, respectively). Depending on the network distribution, TRF, EOP and CRF show different behaviours. There are consistent offsets in the session-wise time series of several Helmert parameters (Tx, Ty, Tz, Rx, Rz) w.r.t. ITRF2014 in the XB network. However, the translation and scale of the XB net- work are more steady than those of the XA network, and thus a more heterogenous network likely benefits transla- tion and scale. The maximum difference between the two legacy networks is 7.1 mm for the Ty component according to the global solutions. In the EOP series, the differences between the wmean values (for the distinct deviation time series w.r.t. IERS 14 C04) of the two legacy networks are 0.2–0.7 mm on the surface of the Earth. It cannot be sim- ply asserted which network is better for EOP determination, because each network has a better agreement with a differ- ent subset of the components. Meanwhile, the VG network shows better agreement with IERS 14 C04 in all the EOP components (except for dY). The XB network still has a dec- lination bias w.r.t. ICRF3 due to the new southern hemisphere stations having only a short observation history, even though the bias became smaller than w.r.t. ICRF2. The XA network

has a rotation (1.7 mm on the Earth surface) in R_1 direction w.r.t. ICRF3, likely due to a North America biased network and the limited visibility of the radio sources on the south- ern hemisphere. The VG network shows inaccurate estimates of the source coordinates due to the restricted number and distribution of the participating stations.

The integration of the three single networks is possible when applying 5 pairs of local ties at the co-located sites (Wettzell, Kokee, and Yebes) and combining the normal equations. The Tx, Ty, and scale of the Helmert parameters in the integrated networks (XAXB and XAXBVG) are in- between the corresponding values of two legacy networks. The integrated networks have less rotation in y and z direc- tion (Helmert parameters) than both legacy networks, while the x-rotation is comparable with the one of the XB net- work. Adding the VG network to the legacy networks did not affect the legacy TRF significantly, but the integration could adjust the station coordinates of the VG network effec- tively. The EOP WRMS values of the integrated networks w.r.t. IERS 14 C04 are similar to those of the legacy net- works, whereas they (except dY) are larger than the WRMS of the VG network. Meanwhile, the wmean values of x-/y- pole and dUT1 of the integrated networks w.r.t. IERS 14 C04 are smaller than for the legacy networks. Adding the VG network to the legacy networks did not show any significant impact in the EOP. The integrated networks still show some rotations (1.2 mm on the Earth surface at the largest) w.r.t. ICRF3, but clearly compensates the adjusted declination bias (D_3 from Fig. 8) from the XA, XB, and VG networks.

The three single networks show different characteristics in terms of TRF, EOP, and CRF, and the integrated network compensates those biases originating from network geometry effectively in most cases. Once a globally balanced VGOS network is available, it will give better geodetic results in the future. To correlate such amount of data, distributed correlation can be the key and therefore distributed computation strategy and supportive software should be developed in more practical and effective ways. Until then, the integration of separate networks, which is already possible because the different networks share common parameters such as EOP and (partly) radio sources, could be the solution to achieve better accuracy and precision. Although it was not discussed in this paper, it should be mentioned here that due to the different frequencies observed with legacy and VGOS networks, and the potential frequency-dependence of the source position and structure, estimating common coordinates may not be applicable to achieve the highest accuracy for some radio sources in the future.

References

Altamimi Z, Rebischung P, Métivier L, Collilieux X (2016) ITRF2014: A new release of the International Terrestrial Reference Frame modeling nonlinear station motions. J Geophys Res Solid Earth 124:6109–6131. https://doi.org/10.1002/2016JB013098

Angermann D, Drewes H, Krügel M, Meisel B, Gerstl M, Kelm R, Müller H, Seemüller W, Tesmer V (2004) ITRS Combination Center at DGFI | a Terrestrial Reference Frame Realization 2003. Deutsche Geodätische Kommission, Reihe B, München

Bizouard C, Lambert S, Gattano C, Becker O, Richard J (2019) The IERS EOP 14C04 solution for Earth orientation parameters consistent with ITRF2014. J Geod 93:621–633

Charlot P and ICRF3 Working Group (2020) The Third Realization of the International Celestial Reference Frame by Very Long Baseline Interferometry. Astron Astrophys 644:A159

Fey AL, Gordon D, Jacobs CS, Ma C, Gaume RA, Arias EF, Bianco G, Boboltz DA, Böckmann S, Bolotin S, Charlot P, Collioud A, Engelhardt G, Gipson J, Gontier A-M, Heinkelmann R, Kurdubov S, Lambert S, Lytvyn S, MacMillan DS, Malkin Z, Nothnagel A, Ojha R, Skurikhina E, Sokolova J, Souchay J, Sovers OJ, Tesmer V, Titov O, Wang G, Zharov V (2015) The second realization of the International Celestial Reference Frame by very long baseline interferometry. Astron J 150(2):58. https://doi.org/10.1088/0004-6256/150/2/58

Gerstl M, Kelm R, Müller H, Ehrnsperger W (2000) DOGS-CS: Kombination und Lösung großer Gleichungssysteme. Interner Bericht Nr. MG/ 01/ 1995/ DGFI, Deutsches Geodätisches Forschungsinstitut, Munich

IUGG (2011) Resolutions adopted by the Council at the XXV IUGG General Assembly, Melbourne, Australia. http://www.iugg.org/resolutions. Accessed 16 May 2020

Kwak Y, Gerstl M, Bloßfeld M, Angermann D, Schmid R, Seitz M (2017) DOGS-RI: new VLBI analysis software at DGFI-TUM. In: Haas R, Elgered G (eds) Proceedings of the 23rd EVGA Meeting, 15–16 May 2017, ISBN 978-91-88041-09-8, pp 212–215

Kwak Y, Bloßfeld M, Schmid R, Angermann D, Gerstl M, Seitz M (2018) Consistent realization of celestial and terrestrial reference frames. J Geod 92:1047–1061

Mayer D, Böhm J, Krasna H (2017) Tropospheric delay modelling and the celestial reference frame at radio wavelengths. Astron Astrophys 606:A143

Mignard F, Klioner S (2012) Analysis of astrometric catalogues with vector spherical harmonics. Astron Astrophys 547:A59

Petrachenko W, Niell A, Corey B, Behrend D, Schuh H, Wresnik J (2012) VLBI2010: Next Generation VLBI System for Geodesy and Astrometry. In: Kenyon S, Pacino M, Marti U (eds) Geodesy for Planet Earth, International Association of Geodesy Symposia 136. Springer, Berlin, pp 999–1005

Titov O, Lambert S (2013) Improved VLBI measurement of the solar system acceleration. Astron Astrophys 559:A95